

Cloning vectors and contamination in metagenomic datasets raise concerns over pangolin CoV genome authenticity

Adrian Jones¹, Daoyu Zhang², Yuri Deigin^{3*} and Steven C. Quay⁴

¹ Independent Bioinformatics Researcher, Melbourne, Australia

² Independent Genetics Researcher, Sydney, Australia

³ Youthereum Genetics Inc., Toronto, Ontario, Canada; [ORCID 0000-0002-3397-5811](https://orcid.org/0000-0002-3397-5811)

⁴ Atossa Therapeutics, Inc., Seattle, WA USA; [ORCID 0000-0002-0363-7651](https://orcid.org/0000-0002-0363-7651)

*Correspondence to: ydeigin@protonmail.com

Abstract

Metagenomic datasets from pangolin tissue specimens have previously yielded SARS-related coronaviruses which show high homology in their receptor binding domain to SARS-CoV-2, suggesting a potential zoonotic source for this feature of the human virus, possibly via recombination (Liu et al. 2019, Lam et al. 2020, Xiao et al. 2020, Liu et al. 2020). Here we re-examine these published datasets. We report that only a few pangolin samples were found to contain coronavirus reads, and even then in low abundance, while other non-pangolin hosted viruses were present in higher abundance. We also discovered extensive contamination with human, rodent, and other mammalian gene sequences, which was a surprising finding. Finally, we uncovered a number of pangolin CoV sequences embedded in standard laboratory cloning vectors, which suggests the pangolin specimens could have been contaminated with sequences derived from synthetic biology experiments. For these reasons, we find it unlikely that the pangolins in question had a coronavirus infection while alive and all current versions of the cited papers claiming a zoonotic infection of pangolins with a SARS-r CoV should be considered unreliable, and either substantial corrections and clarifications should be provided or the papers in question should be retracted.

Introduction

Pangolins, specifically *Manis javanica*, have been proposed as an intermediate host for SARS-CoV-2 by multiple authors because coronaviruses they harbored had a near-identical receptor binding domain (RBD) to that of SARS-CoV-2 (Xiao et al. 2020; Lam et al. 2020; Liu et al. 2020; Zhang, T. et al. 2020). However, the pangolin coronavirus genome sequences with an RBD that is 97% identical at the amino acid level to that of SARS-CoV-2 all stem from a single batch of smuggled pangolins (Chan and Zhan 2020). Researchers have raised the possibility that these pangolins may have been infected by humans (Choo et al., 2020; Wenzel 2020) or another host species (Chan and Zhan, 2020) during trafficking. Alternatively the viral sequences may have arisen through cell culture or other contamination during sequencing. Deigin and Segreto

(2021) note the poor documentation of sample source and usage by Liu et al. (2020) and Xiao et al. (2020) in the derivation of effectively the same pangolin CoV genome (MP789 and GD_1 genome sequences respectively), while Hassanain (2020), Chan and Zhan (2020) and Zhang (2020) note undisclosed source documentation, irregularities and issues with the metagenomic datasets. A complex relationship of undisclosed data sharing and authorship of pangolin CoV datasets was documented by Chan and Zhan (2020), with key dates shown in Table 1.

BioProject/Journal	Paper	Location	Shared data	Oct.19	Nov.19	Dec.19	Jan.20	Feb.20	Mar.20	Apr.20	May 20	June 20	July 20	Aug. 20	Sep.20	Oct.20	Nov.20	Dec.20	Jan.21	Feb.21	Mar.21	Apr.21	May 21	June 21
Paper accept date	Liu et al. 2019	GD		21/10/2019																				
PRJNA573298	Liu et al. 2019	GD																						
Paper accept date	Lam et al. 2020	GX + GD					22/11/2020																	
PRJNA606875	Lam et al. 2020	GX + GD																						
Paper accept date	Xiao et al. 2020	GD																						
PRJNA607174	Xiao et al. 2020	GD																						
Paper accept date	Liu et al. 2019	GD																						
PRJNA607174	Xiao et al. 2020	GD																						
Paper accept date	Xiao et al. 2020	GD																						
PRJNA607174	Xiao et al. 2020	GD																						
Paper accept date	Liu et al. 2020	GD																						
PRJNA686836	Liu et al. 2020	GD																						
Paper accept date	Liu et al. 2021	GD																						
Paper publ. date	Gao et al. 2020	ZJ																						
Paper accept date	Zhang et al. 2020	GD																						
Paper accept date	Li et al. 2020	GD																						
PRJNA610466	Li et al. 2020	GD																						

Table 1. Pangolin paper and dataset publication timeline. Grey: Paper acceptance/publication date; Green: WGS or RNA-Seq dataset publication; Pink: Amplicon dataset publication; Yellow: Amplicon data sequencing. See Supp. Info. 0.1 for the digital version.

Here we review the metagenomic datasets from Liu et al. 2019 (PRJNA573298), Lam et al. 2020 (PRJNA606875), Xiao et al. 2020 (PRJNA607174), Liu et al. 2020 (PRJNA686836) and Li H. et al. 2020 (PRJNA610466) and find serious issues that raise questions as to the validity of the argument that pangolins were infected by a natural SARS-r CoV. This has consequences for SARS-CoV-2 origin analyses as multiple papers have relied on the published pangolin CoV genome sequences GD_1 (Xiao et al. 2020) or MP789 (Liu et al. 2020) or the datasets above for their interpretation (Andersen et al. 2020; Li X et al. 2020b; Niu et al., 2021).

Xiao et al. (2020) and Liu et al. (2020) relied on Liu et al. (2019) datasets for their analyses (Fig. 1). Other pangolin studies have published virus genomes but either relied solely on datasets from Liu et al. (2019) or Xiao et al. (2020) or have not published any metagenomic datasets for independent verification. Zhang, T. et al. 2020 relied solely on datasets (samples Lung08 and Lung07) generated by Liu et al. (2019) (BioProject PRJNA573298). Yang et al. (2021) published a novel murine respirovirus (MRV) strain from pangolin samples published by Xiao et al. (2020) (BioProject PRJNA607174). Gao et al. (2020) identified novel pangolin pestivirus and coltivirus genomes without providing any raw sequencing data.

Li X. et al. (2020) documented analyses of 15 pangolins infected with Malayan pangolin SARS-CoV-2-related coronavirus confiscated from smugglers within the Guangdong Province. Those pangolin samples were collected in March-August 2019 by the Guangzhou wildlife rescue center. Li X. et al. (2020) state that the raw sequencing data was submitted to NCBI as accession number PRJNA640246, however this BioProject could not be found on NCBI as of 9/8/2021. While a correction has been provided in Liu et al. (2021) that addresses issues in Liu et al. (2020)

raised by Chan and Zhan (2020), multiple issues still remain in work by Liu et al. (2019), Lam et al. 2020, Xiao et al. 2020, Liu et al. (2020) and Li H. et al. 2020, which are discussed herein.

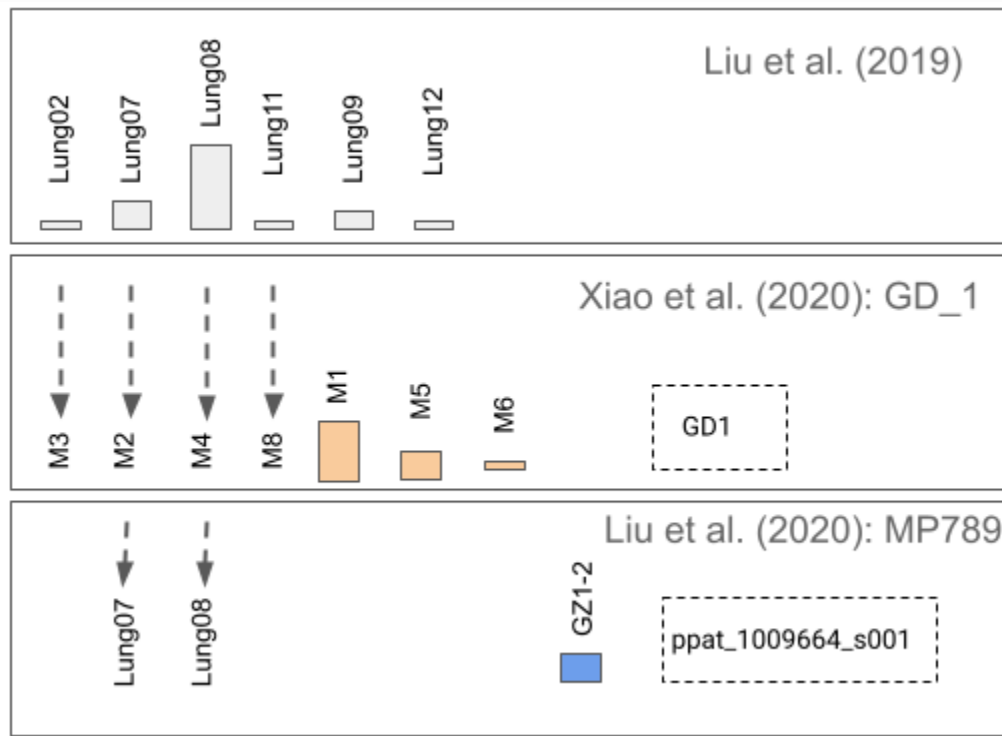


Fig 1. Pangolin samples containing SARS-r CoV reads published by Liu et al. (2019) were used for generating the GD_1 and MP789 genomes by Xiao et al. (2020) and Liu et al. (2020), respectively. Amplicon datasets are indicated by boxes with dashed outlines.

In this paper we make four key observations:

1. The pangolin specimens discussed herein contain frequent and abundant contamination with sequences from a variety of other potential host species, including human and rodent sequences. This makes it impossible to ascertain the viral host in most cases.
2. The few specimens with coronavirus sequences contain evidence of numerous other viruses, many in much higher abundance. This makes it impossible to ascertain that the pangolins died from a coronavirus infection, or were even infected by it while still alive.
3. Many specimens contain large contigs of common laboratory cloning vectors with numerous viral sequences embedded, documenting widespread contamination of the sequencing facility. This makes it impossible to separate a natural zoonotic infection in the pangolins from contamination by results of synthetic biology experiments.
4. Pangolin coronavirus sequences are included in synthetic cloning vectors in the GD1 amplicon dataset (SRR13053879), described as a lung sample by Xiao et al. (2020) supporting the generation of the GD_1 genome (GISAID: EPI_ISL_410721). This suggests the coronavirus sequences identified in the pangolin samples might not stem

from infections of living animals but may have been introduced in the laboratory, possibly inadvertently.

For these reasons, all current versions of the cited papers claiming a zoonotic infection of pangolins with a SARS-r CoV (Liu et al. 2019, Lam et al. 2020, Xiao et al. 2020, Liu et al. 2020) must be considered unreliable, and either substantial corrections and clarifications should be provided or the papers in question should be retracted.

Results

To help with identification of pangolin sample use by multiple authors (Chan and Zhang, 2020, Liu et al. 2021), we used fastv to generate microbial profiles for pangolin metagenomic datasets published by Liu et al. 2019, Lam et al. 2020, Xiao et al. 2020, Liu et al. 2020 (documented in Liu et al. 2021) and Li H. et al. 2020 (Supp. Info. 1.2, 2.2, 3.2, 4.2, 5.1).

We then used bowtie2 to align the same SRAs to selected microbial genomes which were identified with fastv (Fig. 2). We note abundant contamination by non-pangolin hosted virus sequences. While there appears distinct patterns to virus content for each BioProject, numerous similarities are apparent. In particular BioProjects PRJNA573298 (Liu et al. 2019), PRJNA607174 (Xiao et al. 2020), and PRJNA610466 (Li H. et al. 2020) share distinct combinations of viruses, for example *Mus musculus* mobilized endogenous polytropic provirus clone 15 truncated gag-pol polyprotein (gag) and envelope protein (env) genes, complete cds, informally termed ‘MMMEPP’ and Parus major densovirus isolate PmDENV-JL (PmDENV-JL) are common to all three BioProjects, while Simian Virus 40, Enterobacteria phage M13, Parainfluenza virus 5, and Enterobacteria phage DE3 are found in PRJNA607174 (Xiao et al. 2020), and PRJNA610466 (Li H. et al. 2020) but not PRJNA573298 (Liu et al. 2019). A Spearman coefficient matrix plot was generated across all datasets (Supp. Fig. 2), which indicatively showed low positive correlation coefficients between pangolin CoV MP789 and pangolin respirovirus M5 (0.49) and between pangolin CoV MP789 and ‘MMMEPP’ (0.49).

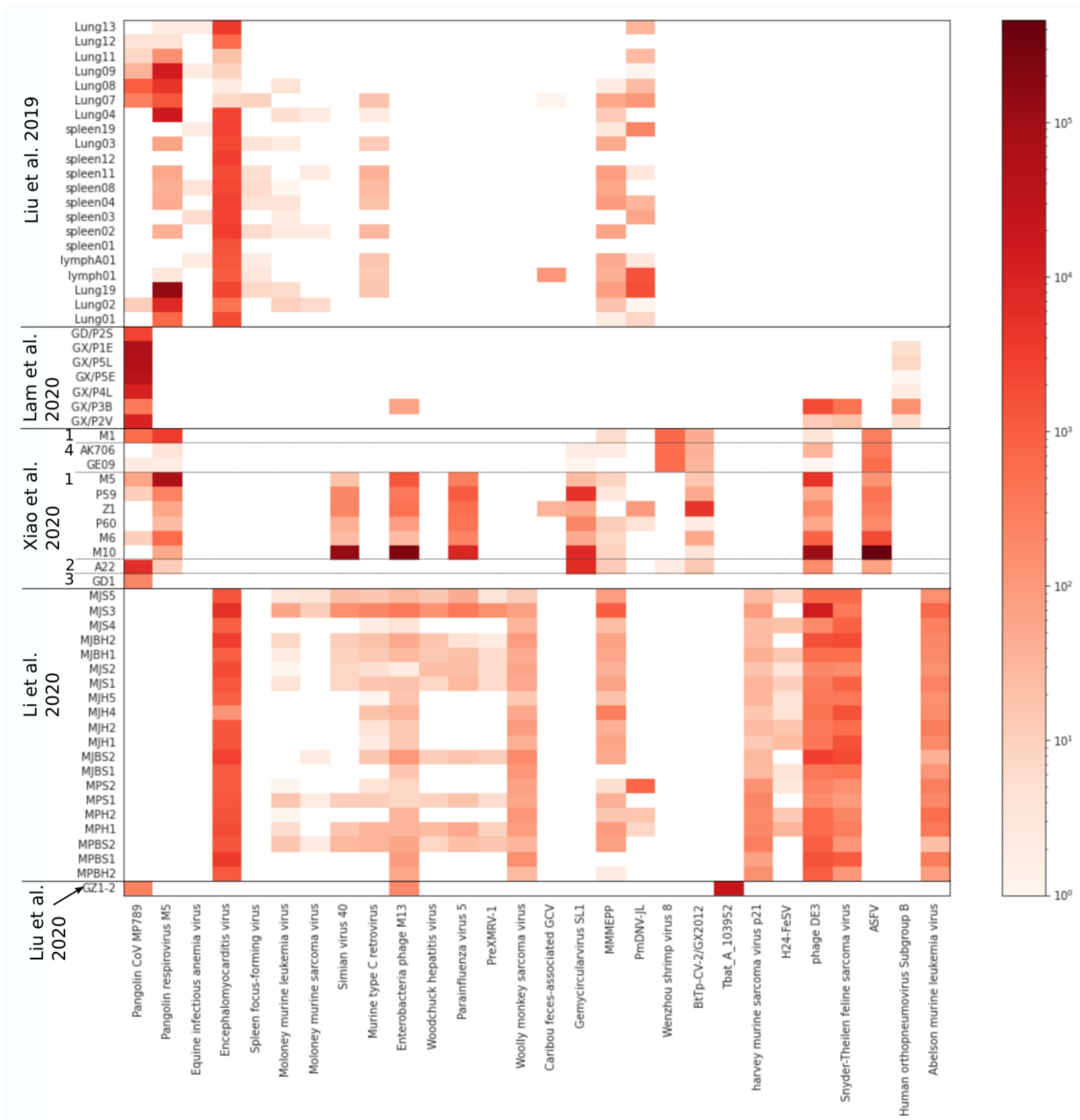


Fig. 2. Virus and microbial sequence read counts (log scale) for samples in Liu et al. (2019) (PRJNA573298), Lam et al. (2020) (PRJNA606875), Xiao et al. (2020) (PRJNA607174) (release stages 1-4), Li et al. (2020) (PRJNA610466) and Liu et al. (2020) (PRJNA686836). Reads aligned using bowtie2. See Supp. Info. 0.2 for dataset information.

Liu et al. 2019 (BioProject PRJNA573298)

Virus taxonomy

We ran a k-mer analysis using fastv (Chen et al. 2020) against the Opengene viral genome k-mer collection for all SRAs in PRJNA573298 (Supp. Info. 1.2). We aligned cleaned reads in each

SRA to the 11 most dominant viral sequences using both bwa mem and bowtie2. We identified numerous misalignments to Sendai virus (NC_001552.1) across the genome, then generated a consensus sequence and ran NCBI BLASTN against against the nucleotide (nt) database to identify pangolin respirovirus isolate M5 (accession MW505906.1) as having the highest homology to these aligned reads (Yang et al. 2021).

A relative read count analysis of total read counts per SRA for the six most abundant identified viral sequences is shown in Fig. 3. The maximum read abundance of pangolin CoV MP789 (MT121216.1) in any sample is slightly lower than for Parus major densovirus isolate PmDENV-JL (NC_031450.1) but significantly lower than Pangolin respirovirus isolate M5 (MW505906.1) and rodent virus but commonly domestic pig hosted Encephalomyocarditis virus (NC_001479.1) read levels, while only two pangolin samples have SARS-r CoV read level above Murine type C retrovirus (NC_001702.1) and Mus musculus mobilized endogenous polytropic provirus clone 15 truncated gag-pol polyprotein (gag) and envelope protein (env) genes (NC_029853.1) informally termed ‘MMMEPP’ and (Supp Figs. S2, S3; Supp. Info. 1.3, 1.4).

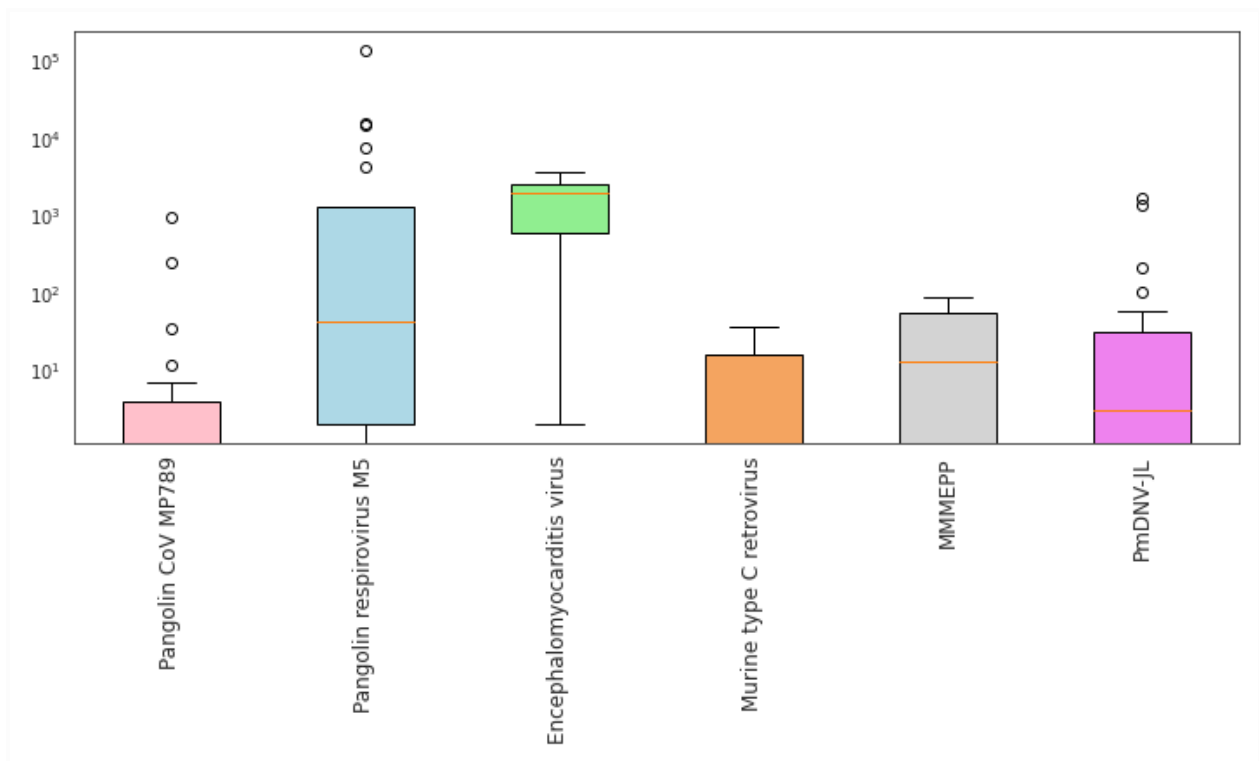


Fig 3. Distribution of total read counts per SRA dataset in PRJNA573298 for the six most abundant viruses identified using fastv. Read counts were identified by aligning each dataset using bowtie2. The Y-axis is log scale. Box extends from the lower to upper quartile values, a red line delineates the median. Whiskers extend to 1.5X of the interquartile range of the data. Outliers are drawn as circles. MMMEPP: *Mus musculus* mobilized endogenous polytropic provirus clone 15 truncated gag-pol polyprotein (gag) and envelope protein (env) genes, complete cds; PmDENV-JL: *Parus major* densovirus isolate PmDENV-JL, complete genome. See Supp. Info. 0.4 for accession numbers. Plotted using Matplotlib.

We then pooled all 21 SRAs of PRJNA573298 and aligned them to the virus sequences identified using fastv (with a replacement of NC_001552.1 by MW505906.1), using bwa mem with default parameters. Similar to results in Fig. 3, two viruses of clear non-pangolin origin had a higher read abundance and genome coverage than pangolin CoV MP789 — namely, *Parus major* densovirus isolate PmDENV-JL (NC_031450.1) (Supp. Fig. S5) and MMMEPP (NC_029853.1). At the same time, Murine type C retrovirus (NC_001702.1) had only 6% fewer reads and 17% lower coverage than MP789.

In BioProject PRJNA573298 (Liu et al. 2019) pangolin coronavirus reads were identified in only 6 of 21 whole-genome sequencing (WGS) SRA datasets (SRR10168374-78 and SRR10168392) with 74.6% of the reads being found in Lung08 (SRR10168377), 21% in Lung07 (SRR10168378) and 2.5% in Lung09 (SRR10168376). No reads were found in dead pangolin sample Lung04 (SRR10168379). Datasets for samples Lung09 (SRR10168376), Lung08 (SRR10168377) and Lung09 (SRR10168378) were pooled and aligned to the pangolin CoV MP789 genome using bwa mem using default parameters (Supp. Fig. S4). Multiple gaps in the coverage of the pangolin CoV MP789 genome (MT121216.1) were found.

De novo assembly and taxonomy

Using fastp cleaned reads, we generated contig sequences by *de novo* assembly using MEGAHIT. We used MagicBLAST against a local copy of the nt database to classify sequence identities (Fig. 4; Supp Fig. S6).

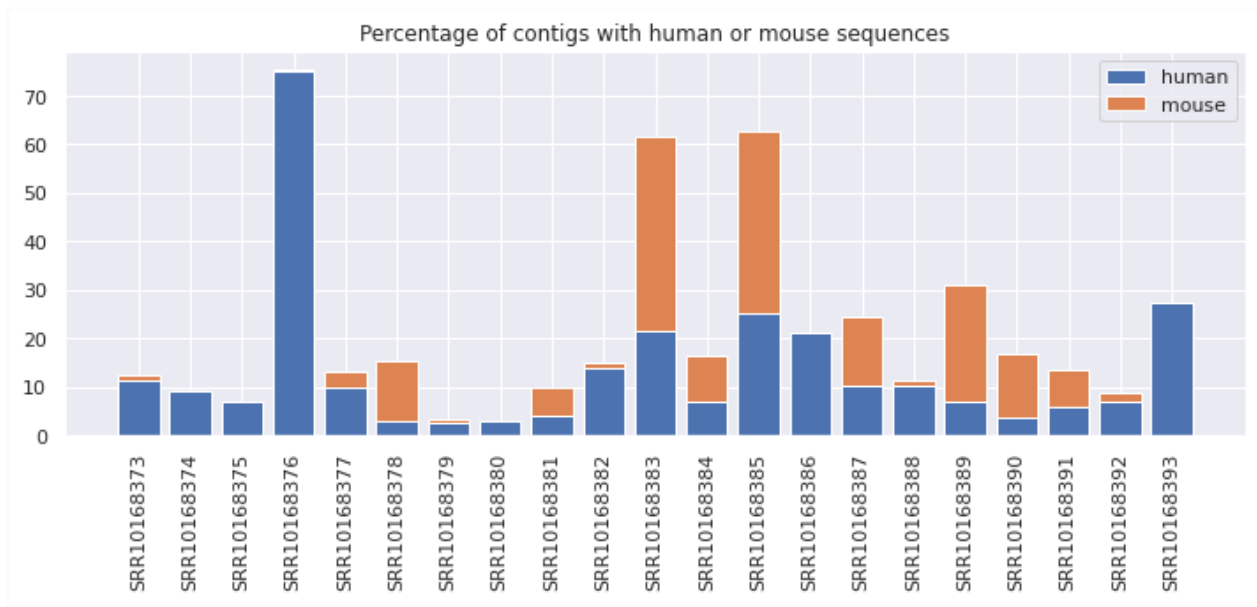


Fig. 4. Percentage of contigs per SRA in PRJNA573298 identified using MagicBLAST against the nt database with description including the terms 'human' or '*Homo Sapiens*' (human) or '*Mus musculus*' (mouse).

We then aligned cleaned reads to *Homo sapiens*, *Manis pentadactyla*, *Manis javanica*, and *Mus musculus* mitochondrial genomes using bowtie2 (Supp. Info. 1.3). Multiple SRAs have high levels of human and or rodent sequence contamination. Indeed, Lung09, Spleen11 and Spleen04 have combined *Mus musculus* and human sequence matching contig counts higher than pangolin matching contigs. A summary of taxonomic analysis of selected samples in PRJNA573298 is shown in Table 2.

Sample	MP789	P/M mito.	P/H mito.	STAT <i>Muroidea</i>	STAT <i>Catarrhini</i>	STAT Hom.	Contigs Mus.	Contigs human
Lung01			4762:1			40%	0.21%	27.30%
Lung02	12	28:1	4:1	8%		4%	1.85%	6.80%
Lung03		3:1	3:1				5.8%	4.20%
Lung07	258	76:1	4749:1	11%		3%	3%	12.30%
Lung08	984	38:1	6:1	12%		7%	3.25%	9.86%
Lung09	35		417:1			65%	0.22%	75%
Lung11	7		46557:1	1%			0.18%	6.83%
Lung12	4		61:1		23%		0.06%	9.25%
LymphA01		21:1	1700:1	21%			24.1%	7%
Lymph01		94:1	4629:1				13.3%	3.62%

spleen02		206:1	176:1	31%		4%	14.25%	10.31%
spleen03			67:1			44%	0.09%	21.06%
spleen04		129:1	121:1	36%		4%	37.46%	25.32%
spleen08			92:1	12%	1%		9.55%	6.88%
spleen11		220:1	211:1	28%	4%		40.05%	21.64%

Table 2. Analyses of selected samples in PRJNA573298. MP789: counts of reads aligned to pangolin CoV MP789 using bowtie2; P/M mito.: ratio of reads aligned to *Manis pentadactyla*+*Manis javanica*/*Mus musculus* mitochondrial genomes; P/H mito. ratio of reads aligned to *Manis pentadactyla*+*Manis javanica*/*Homo sapiens* mitochondrial genomes; STAT *muroidea*: NCBI STAT percentage of *Muroidea*+*Mus*+*Mus musculus*+*Rattus norvegicus*; STAT *Catarrhini*: NCBI STAT percentage of *Catarrhini*; STAT Hom.: NCBI STAT percentage of *Homininae*+*Homo Sapiens*; Contigs Mus.: percent *de novo* assembled contigs matching *Mus musculus* sequences; Contigs human: percent *de novo* assembled contigs matching human sequences.

Furthermore, we identified 150 contigs with matches to synthetic vectors (Supp. Info. 1.7, Supp. Fig. S9), and 260 contigs matching (non-retroviral) virus sequences (Supp info. 1.8, Supp. Fig. S10). Contigs from Lung08 (SRR10168377) and Lung09 (SRR10168376) contained the highest amounts of vector sequences, while Lung08 (SRR10168377) and Lung07 (SRR10168378) contained the highest number of contigs matching virus sequences.

We then added counts of human and mouse sequence matching contigs to a table of aligned virus read counts and generated a Spearman correlation coefficient matrix plot (Supp. Fig. S11). Moderate positive correlation was found between MP789 read counts and pangolin respirovirus M5 read counts (0.54) and between MP789 read counts and mouse contig counts (0.6).

We identified contigs that were classified as vector and virus using MagicBLAST against a local copy of the nt database. We then ran local BLAST against the nt database for these contigs (Supp. Info. 1.7 and 1.8). Finally, we aligned the contigs to a local set of virus sequences downloaded from the Genome Sequence Archive using minimap2 (Supp. Info. 1.9). We found multiple contigs matching the following virus sequences: Synthetic Vaccinia virus clone GLV-1h68, XMRV-like mouse endogenous retrovirus mERV-XL, Infectious bronchitis virus isolate YN/V90/2012 nucleocapsid protein-like (N) gene, Porcine epidemic diarrhea virus isolate GER/L03207/2019, Avian orthoavulavirus 1, Rous sarcoma virus, Equine infectious anemia virus, Moloney murine sarcoma virus, as well as pangolin coronavirus isolate MP789 and multiple cloning vectors including pcDNA3.1_+ (MN996867.1) (Supp. Info. 1.9). Noting that Zhang (2020) had identified pcDNA3.1_+ in BioProject RJNA607174, we then aligned pooled reads from the 21 SRAs and found 5530 reads mapped to MN996867.1, generating a 73.12% coverage of the vector sequence (Supp. Figs. S12, S13). Abundant misaligned read sections were evident in the alignment, thus the vector present in the above SRAs may be a related or a modified version.

Lam et al. 2020 (BioProject PRJNA606875)

The datasets for the Lam et al. 2020 study of 6 Guangxi pangolin samples and one Guangdong pangolin scale were registered on NCBI on 15/2/2020 and published on 26/3/2020. The SRA datasets consist of four amplicon sequencing datasets (SRR11093266-9) and three RNA-Seq datasets (SRR11093265, SRR11093270-1) (Supp. Info. 0.2). However, the RNA-Seq dataset GD/P2S (SRR11093265) has been heavily filtered, with all non-coronavirus reads filtered out, leaving a dataset of only 2,633 reads. This compares with 55,384,421 reads for sample GZ1-2 (SRR13285085) by Liu et al. 2020, also sequenced by a NextSeq 550 instrument. We further note that sample GD/P2S (SRR11093265) was sequenced on two different machines “@NDX550382_RUO” (NextSeq 550) and “@NB501248AR” (Unknown platform). Furthermore GD/P2S is the only dataset in PRJNA606875 without a description of an isolation source or a library prep procedure.

Hassanin (2020) identified 11 reads exactly matching SARS-CoV-2 and four reads with only a single mutation difference in the GD/P2S dataset (SRR11093265). Here we undertook a BLASTN search of SARS-CoV-2 Wuhan-Hu-1 (NC_045512.2) against the GD/P2S dataset (SRR11093265). We found 83 reads of 75-nt length with an identical match and 132 reads of 75-nt length with a single nucleotide difference (Supp. Fig. S14). We then aligned the GD/P2S dataset to GD_1 (EPI_ISL_410721) and SARS-CoV-2 Wuhan-Hu-1 (NC_045512.2) using bwa-mem2 and further identified 4 reads 44-53 nucleotides long with an exact match to SARS-CoV-2 Wuhan-Hu-1. One 49-nt exactly matching read contained the SARS-CoV-2 furin cleavage site sequence ‘CGGCGGGCACGT’.

In sample GX/P2V (SRR11093271), which used Vero-E6 cell line culture for pangolin CoV isolation, after alignment to SARS-CoV-2 Wuhan-Hu-1 (NC_045512.2) using bowtie2, we identified 20 reads of 70-95 nucleotide length (70 nucleotides was used as a minimum cutoff) with an exact match to SARS-CoV-2 (NC_045512.2) (Supp. Info. 0.3 ids 30-49) clearly indicating SARS-CoV-2 contamination of a second dataset in this BioProject.

As the SARS-CoV-2 reads were only found in the GD/P2S dataset (SRR11093265) which was the only SRA in this project to use a NextSeq 550 instrument, and in sample GX/P2V (SRR11093271) which used Vero-E6 cell culture, we believe that the most parsimonious explanation for this observation is that the SARS-CoV-2 reads were derived from contamination. Given that the GD/P2S dataset contains contamination with SARS-CoV-2 reads, and has had an estimated 99.995% of the all reads filtered out from the original dataset (other than SARS-r CoV reads), this dataset cannot be relied upon as a true metagenomic sample supporting a novel Guangdong pangolin CoV.

Using fastv, we identified several virus sequences in each of the SRA datasets (Supp. Info. 2.2), and then aligned each SRA dataset in the project to these viral genomes (Supp. Info. 2.4, 2.5, Supp. Fig. 15, 16). All datasets except GD/P2S (SRR11093265) contained traces of Influenza A virus while GX/P3B (SRR11093270) contained both Enterobacteria phage DE3 and Enterobacteria phage M13 reads.

After *de novo* assembly of each SRA in the project, we analysed each contig against a local copy of the nt database using MagicBLAST (Supp. Fig. S17-20). In sample GX/P3B (of the two RNA-Seq datasets which were not heavily filtered), we identified 105 and 102 contigs matching human and *Canis lupus* sequences respectively as well as cloning vectors pColE-AT and pColE-FRT (Supp. Info. 2.3).

Xiao et al. 2020 (BioProject PRJNA607174): Pangolin CoV GD_1

Metagenomic datasets were released by Xiao et al. 2020 in 4 stages (Table 1). WGS datasets used for generating the GD_1 genome (GISAID: EPI_ISL_410721) were published on 22/4/2020. An undocumented WGS dataset was published to NCBI on 22/6/2020. Primer-based amplicon sequences were uploaded to NCBI on 17/11/2020 and finally two WGS datasets which were sequenced on the same Illumina machine and run as sample M1 were uploaded to NCBI on 16/6/2021 (Supp. Info. 0.2).

Microbial signature of datasets

We ran a k-mer analysis using fastv (Chen et al. 2020) against the Opengene viral genome k-mer collection for all SRAs in PRJNA607174 (Supp. info 3.2). We then aligned cleaned reads to each of the microbial sequences identified using bowtie2 (with a replacement of NC_001552.1 by MW505906.1) (Supp. Info. 3.3, 3.4; Supp Fig. S21, S22). Higher read abundance than reads aligning to pangolin CoV MP789 with similar high coverage as for MP789 was found for alignments to pangolin respirovirus isolate M5 (MW505906.1), Parainfluenza virus 5 (NC_006430.1) and Gemycircularvirus SL1 (NC_026818.1). 100% coverage but with 30% lower reads than alignment to pangolin CoV MP789 was found in sample Z1 for alignment to bat-associated cyclovirus 9 isolate BtTp-CV-2/GX2012 (NC_038399.1). A c. 94% coverage of Wenzhou shrimp virus 8 strain shrimp14543 hypothetical protein gene (NC_032852.1) was found in sample AK706 (Supp info. 3.3, 3.4). The total read count for each SRA for the eleven most common viruses was then plotted to show the relative count distribution (Fig. 5).

Similarly to the count distribution for pangolin CoV MP789 seen in data from Liu et al. 2019 (PRJNA573298), multiple contaminating sequences have a higher mean and maximum read count. Notably, African Swine Fever virus sequences, which were found to be part of synthetic vector constructs, were found in higher abundance than pangolin CoV MP789 in this BioProject.

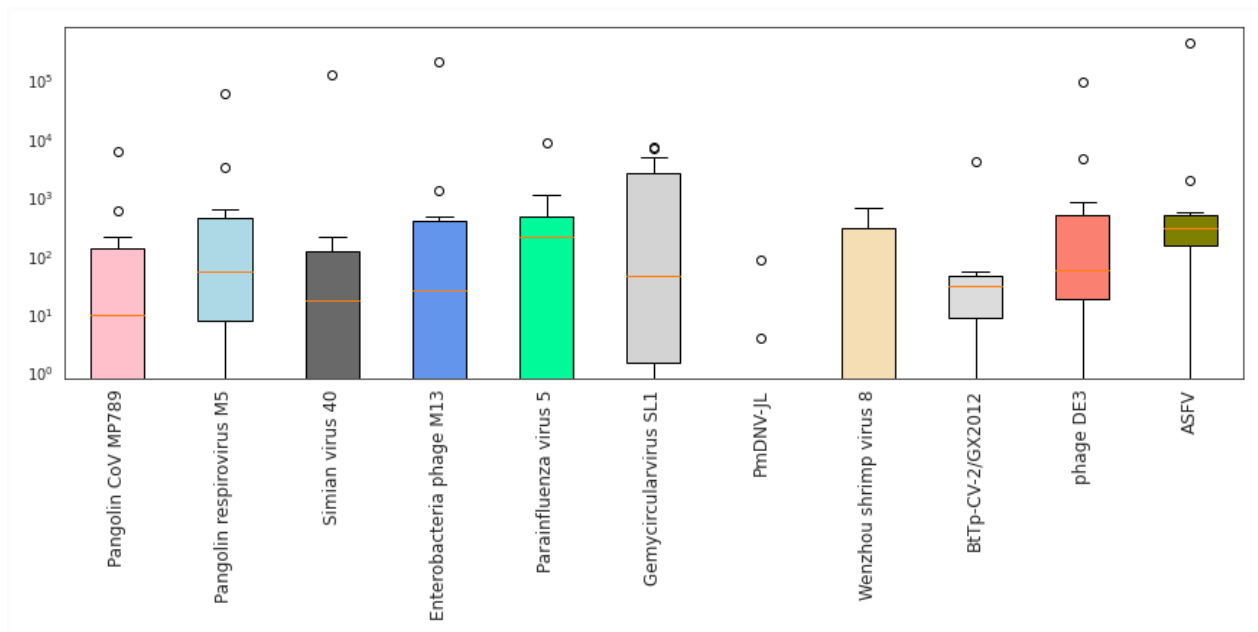


Fig. 5. Distribution of total read counts per SRA dataset in PRJNA607174 for the eleven most abundant viruses identified using fastv. Read counts identified by aligning each dataset using bowtie2. The Y-axis is log scale. Box extends from the lower to upper quartile values, a red line delineates the median. Whiskers extend to 1.5X of the interquartile range of the data. Outliers are drawn as circles. Plotted using Matplotlib. See Supp. Info. 0.4 for full names and accession numbers.

We then used counts of reads aligned to selected virus genomes using bowtie2 as well as counts of *de novo* assembled contigs matching human or *mus musculus* sequences and generated a Spearman coefficient matrix for all SRAs in PRJNA607174 with the exception of amplicon dataset GD1 (Supp Fig. S23). We found high positive correlation between pangolin CoV MP789 and Enterobacteria phage M13 read counts (0.87); and between pangolin CoV MP789 read counts and mouse contig counts (0.81). Moderate positive correlations were found between pangolin CoV MP789 to Gemycircularvirus SL1 and pangolin CoV MP789 to *Mus musculus* mobilized endogenous polytropic provirus clone 15 truncated gag-pol polyprotein (gag) and envelope protein (env) genes, complete cds (0.67 and 0.62 respectively) (Supp Fig. S23).

Sample A22

Sample A22 (SRR12053850) was submitted to NCBI on 19/6/2020, over a month after WGS dataset release on 22/4/2020 and paper publication on 7/5/2020. The sample was sequenced on a different machine id (“A00151”) to the other WGS datasets (Supp. Info. 0.2) in this BioProject and contains the highest Pangolin CoV read count of all WGS datasets in the project. Indeed, it is the only sample of the 16 in PRJNA573298 and 10 in PRJNA607174 containing Sendai-related virus reads (MW505906.1) where pangolin CoV reads exceed Sendai-related virus read counts. However, as Chan and Zhan (2020) note, Xiao et al. (2020) declare that RNA sequencing from

nine pangolin lung samples, seven of which had reads mapped to SARS-CoV-2 (MN908947), were used to generate the GD_1 genome (GISAID: EPI_ISL_410721). The nine pangolin lung samples were specified in Xiao et al. (2020) Extended Data Table 3, and do not include sample A22 and as such this sample will not be used here for GD_1 genome analysis.

We aligned each SRA in BioProject PRJNA607174 to the Pangolin CoV MP789 genome using bwa mem. Read coverage is shown in Fig 6. Sample A22 had the best coverage of the WGS datasets.

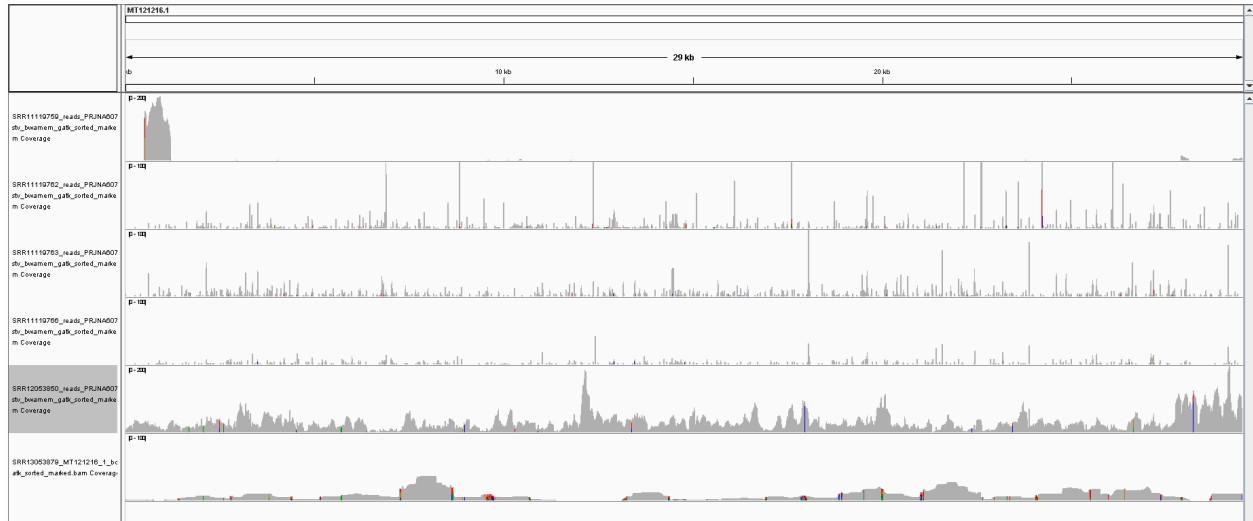


Fig. 6. Read coverage plots for Xiao et al. (2020) samples (top to bottom) M1 (SRR1119759) (0-200 scale), M5 (SRR1119762) (0-100 scale), P59 (SRR1119763) (0-100 scale), M6 (SRR1119766) (0-100 scale), A22 (SRR12053850) (0-200 scale) and GD1 amplicons (SRR13053879) (0-100 scale) aligned to MP789 (MT121216.1), plotted in IGV.

We pooled the nine pangolin samples specified in Xiao et al. (2020) Extended Data Table 3 and aligned the combined dataset to the GD_1 genome using bowtie2 (Table 3, Supp Fig. Xiao_GD1). Reads did not cover the full genome and mapping depth was poor with only 56.6% coverage at a read depth of 4X and 5.4% at 30X, a recommended depth for robust genome sequencing (Hassanin, 2020; Sims et al., 2014).

N	Avg depth	Median	Coverage%	Cov 4x %	Cov 10x %	Cov 30x %	Cov 100x %
1955	10.74	5	90.63	56.6	22.09	5.39	1.78

Table 3. Coverage statistics for alignment of nine pangolin samples specified in Xiao et al. (2020) Extended Data Table 3 to the GD_1 genome using bowtie2. Statistics calculated using bamdst v1.0.9 and bamstats v1.25. N: number of reads mapped. Average depth and median depth calculated for mapped regions only.

Amplicon dataset

In the third data release by Xiao et al. (2020), GD1 amplicon sequence (SRR13053879) was published on NCBI on 17/11/2020, after Chan and Zhan (2020) noted that data supporting gap coverage had not been provided by Xiao et al. 2020. We checked for standard adapter sequences using FastQC and searched for the presence of the first 12/13nt of standard adapter sequences but did not detect the presence of adapter sequences. We then ran fastp to filter the dataset with 240 of 240 reads passing filtering. We aligned the GD1 amplicon reads to the GD_1 genome (EPI_ISL_410721) using bwa mem with default parameters. The aligned amplicon reads as well as raw read coverage is shown in Fig. 7, with a zoomed in view of the 3' end shown in Fig. 8.

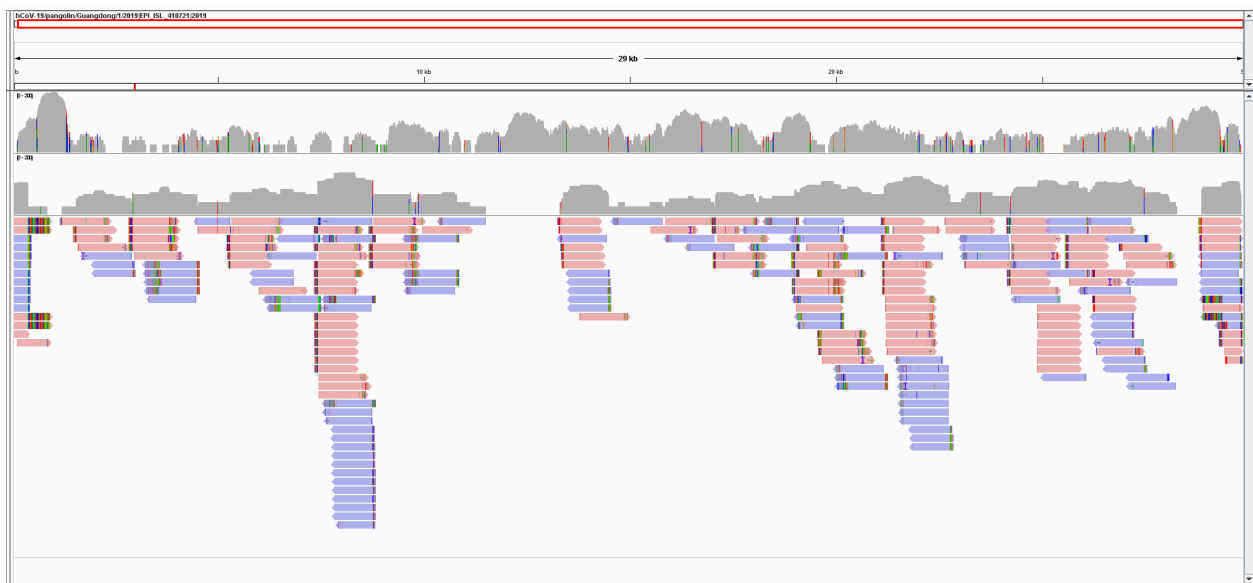


Fig 7. Pooled reads from SRAs in Xiao et al. (2020) Extended Table 3 coverage aligned to the GD_1 genome with bowtie2 (grey, upper track, 0-200 log scale); GD1 amplicon reads aligned to GD_1 genome with bwa mem: coverage track (grey, 0-200 log scale), and read track, coloured by read direction (pink/blue) and mismatched bases (strong colours). Gaps in the raw read coverage are covered by amplicon reads. Displayed in IGV.



Fig 8. Contigs from *de novo* assembly of pooled reads from SRAs in Xiao et al. (2020) Extended Data Table 3 coverage aligned to GD_1 genome with bowtie2 (top two tracks) and GD1 amplicons (SRR13053879) aligned to the GD_1 genome (EPI_ISL_410721) (bottom two tracks), zoomed in at the 3' end. GD_1 sequence ends at 29825 nt (indicated by the right-hand edge of the grey coverage track).

10 reads in the GD1 amplicon sequence dataset extended downstream past the 3' end of the GD_1 genome. Read id '12' (Supp. Info. 0.3, 14th read from top at 3' end in Fig. 8), one of the two 3'-most reads in Fig. 8 above was analysed with addgene. The GD_1 sequence terminates at 538 nt in this read sequence.

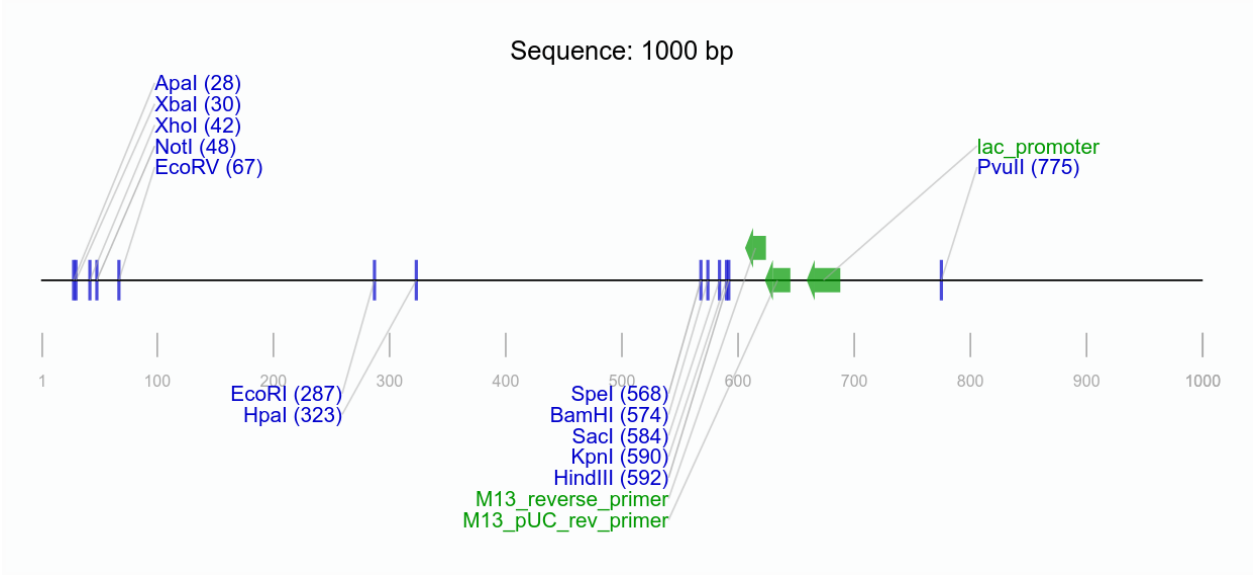


Fig. 9. Amplicon read '12' (Supp. Info. 0.3) plotted in addgene sequence analyzer.

The part of the read sequence outside the GD_1 genome (539-1000 nt) was then analysed using NCBI BLASTN against the nt database using default settings (Supp. Fig. S24) with highest alignment score to multiple cloning vectors (including Cloning vector pVMG0193_Cq-Rpl40-Cas9) with a 462 of 463 nt match and cloning vectors pXF20pemIK-GW, pPS2305, pCR2.1-sacB with a 457 of 457 nt match (Supp Fig. S25). The 81-nt misaligned section at the 5' end of the read was also analysed using NCBI BLAST against the nt database, resulting in a match with a 100% identity to a 75-nt section of cloning vectors pEASY-tub/hptII, pEASY-tub/aadA, pEASY-tub/ble and pEASY-T1 (Supp Figs S26, S27).

GD_1 amplicon reads aligned to the 5' end of the GD_1 genome are shown in Fig. 10 below. Notably, 13 amplicon reads extend upstream of the GD_1 genome sequence, with 9 extending over 500 nucleotides upstream. Also notable is that the amplicons cover a ~120-nt gap in pooled read coverage at the 5' end of the GD_1 genome sequence.

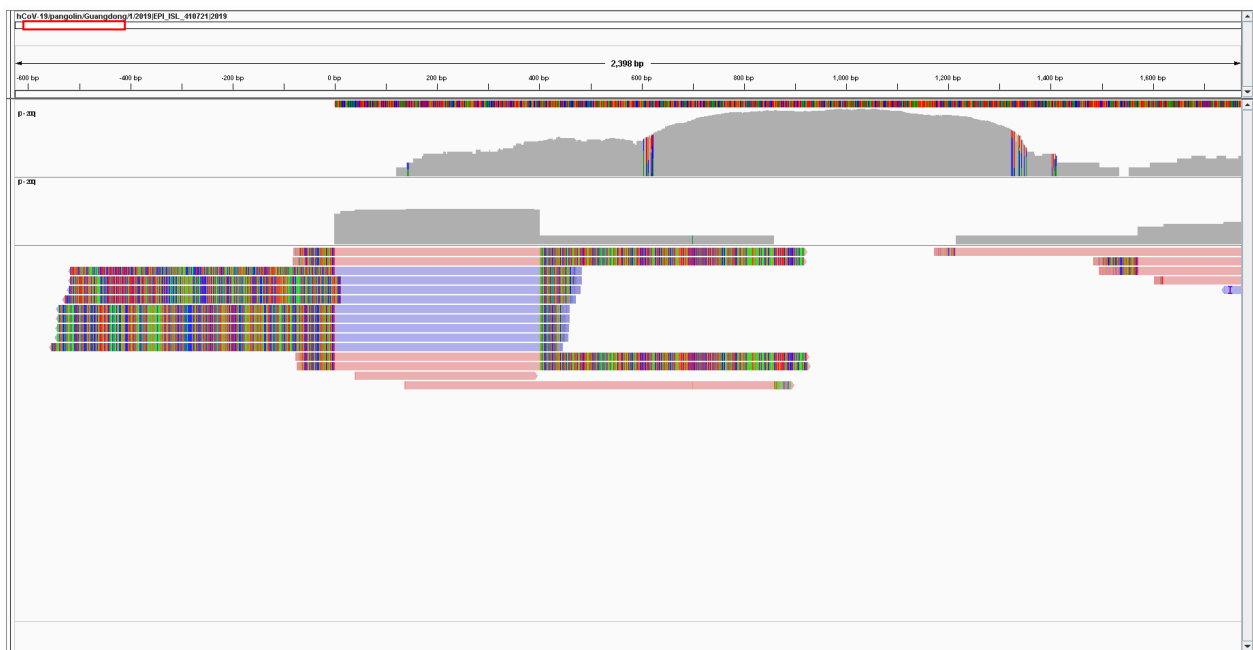


Fig. 10. Pooled reads from SRAs in Xiao et al. (2020) Extended Data Table 3 coverage aligned to GD_1 genome with bowtie2 (grey, top track, 0-200 log scale); GD_1 amplicon reads aligned to GD_1 genome with bwa mem: coverage track (grey, 0-200 log scale), and read track, coloured by read direction (pink/blue) and mismatched nucleotides (strong colours). Zoomed in to the 5' end of the GD_1 genome (-600 to 1650 nt). Displayed in IGV.

The 5' end of read id '25' (Supp. Info. 0.3) (5' most read Fig. 10 above) which was outside of the GD_1 genome alignment (1-554 nt) was analysed using NCBI BLASTN against the nt database resulting in a match with 100% identity to the cloning vectors pEASY-T1 (EU233623.1), pEASY-tu/hptII, pEASY-tu/aadA and pEASY-tu/ble (Supp. Fig. S28).

We then analysed the 59-nt misaligned section of the 3' end of read id '21' in Supp. Info. 0.3 (7th read from top in Fig 10, same read direction and matching 5' end sequence as read id '25') using BLAST against the nt database and found a 100% match for a 50-nt section of cloning vectors pEASY-tub/hptII, pEASY-tub/aaadA, pEASY-tub/ble, and pEASY-T1. We then spliced the synthetic section of the two read ids '25' and '21' (Supp. Info. 0.3) to form a more complete synthetic vector sequence (Fig. 11).

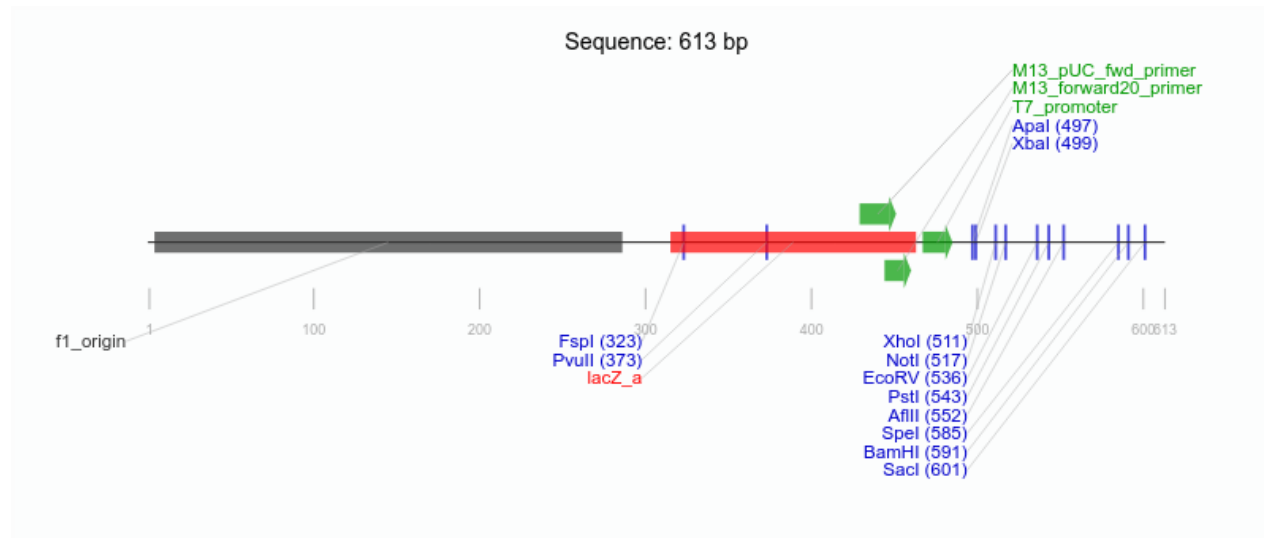


Fig. 11. Misaligned ends of read ids '21' and '25' (Supp. Info. 0.3) were spliced and plotted in the Addgene sequence analyzer.

The spliced sequence was then analyzed with NCBI BLASTN against the nt database and a 99% match (603 of 604 nucleotides) was found to cloning vector pEASY-T1 (Supp. Fig. S29, S30; Supp. Data 'SRR13053879_pEASY-T1_from_spliced_read_ids_21_25.fa')

We further note that a large amount of reads in the amplicon dataset GD1 (SRR13053879) exhibit a distinct pattern of misalignment to the GD_1 genome sequence at either the 5' or 3' ends or both (Supp. Fig. S31). We found that 90% of the 240 amplicon reads had read ends where >14-nt long contiguous sections misaligned to the GD_1 genome (79 were misaligned at both ends, 70 were misaligned at only the 5' end while 67 misaligned at the 3' end only). We used a local BLAST search against the nt database and identified that 85 of the misaligned read ends matched the cloning vector pEASY-tub/hptII, 4 matched pEASY-tub/aaadA and 1 matched vector pEASY-tub/ble.

After *de novo* assembly of the SRR13053879 amplicon dataset, two contigs "k79_3" and "K79_5" were identified with M13 primer sequences and found to match multiple cloning and expression vectors (Supp. Fig. S32-S39).

In all, 48 amplicon reads had either ‘M13R’ or ‘M13F’ in the read name. We found that 11 amplicons that had ‘M13F’ in their name had complete M13_reverse_primer, M13_pUC_rev_primer, lac_promoter and NotI restriction enzyme sequences. While one had complete M13_reverse_primer, M13_pUC_rev_primer and NotI restriction enzyme sequences. 7 reads which had ‘M13R’ in their name had complete T7_promoter and NotI restriction enzyme sequences.

De novo assembly

After *de novo* assembly of each WGS SRA in PRJNA607174, each contig was analysed against a local copy of the NCBI nt database using MagicBLAST with default settings. Contigs with the highest similarity to certain animal types, as well as to viruses, vectors and mycoplasma were grouped by SRA and counted (Supp. Fig. S40) with highest non-pangolin matching contig percentages shown in Fig 12.

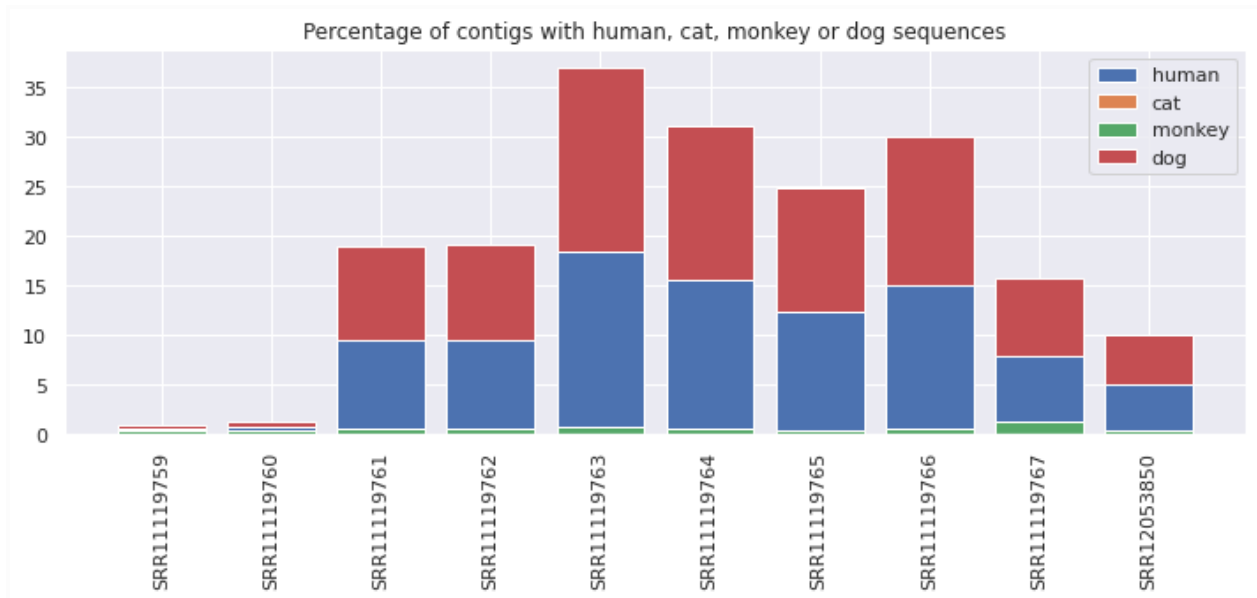


Fig. 12. *De novo* assembled contigs for each WGS SRA in PRJNA607174 were analyzed against the nt database using MagicBLAST, highest non-pangolin matching contig percentages are shown.

Pangolin RNA/DNA sequences were the most common; however, up to 18.5% of contigs had a highest match to *Canis lupus* (SRR11119763) and up 13.4% best matched human DNA/RNA sequences (SRR11119760) (Supp. Fig. S41-45). A taxonomic analysis using the NCBI STAT tool revealed reads in sample M1 (SRR11119759) and AK706 (SRR11119760) to be comprised of 17% and 23% human genetic sequences, respectively (Supp. Info. 3.1).

We next identified contigs matching viruses (excluding retroviruses) and vectors (Supp. Info. 3.5; 3.6). We identified 833 synthetic vector contigs (Supp Fig. S46). Cloning vectors, mammalian expression, Human ORfeome and Expression vector types were the most abundant.

Sample M10 (SRR11119767) had by far the largest count of synthetic vector contigs. We further identified 777 contigs containing virus genome sequences (Supp. Fig. S47). Contigs with Wenzhou shrimp virus 8 strain shrimp14543 hypothetical protein gene (KX883984.1) were the most abundant, followed by Mammalian orthorubulavirus 5 strains (MG921602.1, MH362816.1, MH370862.1, KX100034.1). 8 contigs containing pangolin CoV MT121216.1 sequences were found, 7 in sample A22 (SRR12053850) and one in sample M1 (SRR11119759).

We further identified contigs with common synthetic primer/promoter sequences, then identified open reading frames and translated these to proteins and analysed either against a local copy of the nr database or using the online NCBI nr database (Supp. Info. 3.7). We recovered protein codings for 51 translated ORF's, with 31 having sequences coding for African Swine Fever virus proteins. Large contigs containing a Porcine circovirus 2 capsid protein from sample M5 (SRR11119762), and African Swine Fever Virus proteins (from sample Z1 (SRR11119764)) were plotted in Addgene (Supp. Fig. S48, S49). We note that several recent ASFV related publications by South China Agricultural University (SCAU) affiliated authors (which published BioProject PRJNA607174): *in vitro* viral RNA transcription inhibitor research (Huang, et al. 2021), a vaccine overview (Wu et al. 2020), and rapid detection methodology (Bai et al. 2019). SCAU affiliated authors have also previously published Porcine circovirus 2 related research (Zhai et al 2014; Wei et al. 2019; Zhai et al 2017).

We used minimap2 to align the contigs against a set of virus sequences downloaded from the Genome Sequence Archive (Supp info. 3.8). Multiple contigs aligned to: African swine fever virus, Transmissible gastroenteritis virus, Hepatitis C virus, Cowpox virus, Simian virus 40, Moloney murine sarcoma virus, Rous sarcoma virus, Avian orthoavulavirus 1, Canine coronavirus, Porcine epidemic diarrhea virus, Infectious bronchitis virus, XMRV-like mouse endogenous retrovirus, Synthetic Vaccinia virus clone GLV-1h68, as well as pangolin coronavirus isolate MP789 and numerous cloning vectors.

Li H. et al. 2020 (BioProject PRJNA610466)

Li et al. (2020) specify in materials and methods that fourteen skin samples of *M. javanica* animals were collected from the Guangdong Provincial Wildlife Rescue Centre (PRJNA610466). However, the date when the samples were collected was not provided. The authors also did not specify if the samples were sourced from the same batch of pangolins sampled by Liu et al. (2019) or if data from BioProject PRJNA573298 (Liu et al. 2019) was used. We found that the Illumina read headers showed that the same machine id was used "@A00184" (runs 448 and 449) as in the 9 SRAs from Liu et al. (2019) BioProject PRJNA573298 (runs 351 and 352) (Supp info. 0.2).

Using fastv we identified several virus genome sequences common to BioProject PRJNA573298 and PRJNA610466. We aligned each SRA in BioProject PRJNA610466 to the more abundant viruses and microbes (Supp info. 4.2, 4.3, 4.4, Supp Fig. S50, S51). We found 1030 reads in sample MJS3 (SRR11306689) for 91% coverage of *Mus musculus* mobilized endogenous polytropic provirus clone 15 truncated gag-pol polyprotein (gag) and envelope protein (env) genes, 779 reads and 68% coverage of Parus major densovirus isolate PmDENV-JL (NC_031450.1) in MPS2 (SRR11306700), and 5711 reads in MJS3 (SRR11306689) covering the same ~130-300 nucleotide region of Encephalomyocarditis virus (NC_001479.1) as per Lung13 in Liu et al. 2019.

We then used counts of reads aligned to selected virus genomes using bowtie2 as well as counts of *de novo* assembled contigs matching human or muine sequences and generated a Spearman coefficient matrix for all SRAs in PRJNA610466 (Supp Fig. S52). We found high positive correlation between Woodchuck Hepatitis virus (the WPRE of which is widely used in gene transfer vectors) counts and human contig counts (0.85); high correlation between mouse contig counts and multiple murine viruses; and very high positive correlations between Simian Virus 40 and Hardy-Zuckermann 4 feline sarcoma virus (H24-FeSV) kit oncogene (0.95). Similarly to PRJNA573298, but unlike PRJNA607174, Parus major densovirus isolate PmDENV-JL did not exhibit strong correlation to other viruses or contig counts (Supp Fig. S52).

De novo assembly

After *de novo* assembly of each RNA-Seq SRA in BioProject PRJNA610466, each contig was analysed against a local copy of the NCBI nt database using MagicBLAST with default settings. Contigs with highest similarity to certain animal types, as well as to viruses, vectors and mycoplasma were grouped and counted (Supp. Fig. S53). Sample MJS3 (SRR11306689) was clearly anomalous compared with the other SRAs, having more *Mus musculus* contigs than pangolin ones, as well as a high number of human contigs and significant amount of *sus scrofa* contigs (Supp. Fig. S53,S55, S56). MJS3 also had the highest number of synthetic vector contigs (Supp. Fig. S57) and virus contigs (Supp. Fig. S58). Using taxonomic classification with NCBI STAT, the most anomalous feature of MJS3 compared with other samples in the project is the 14% bacterial content, 7x more than any other sample (Supp. Info. 4.1).

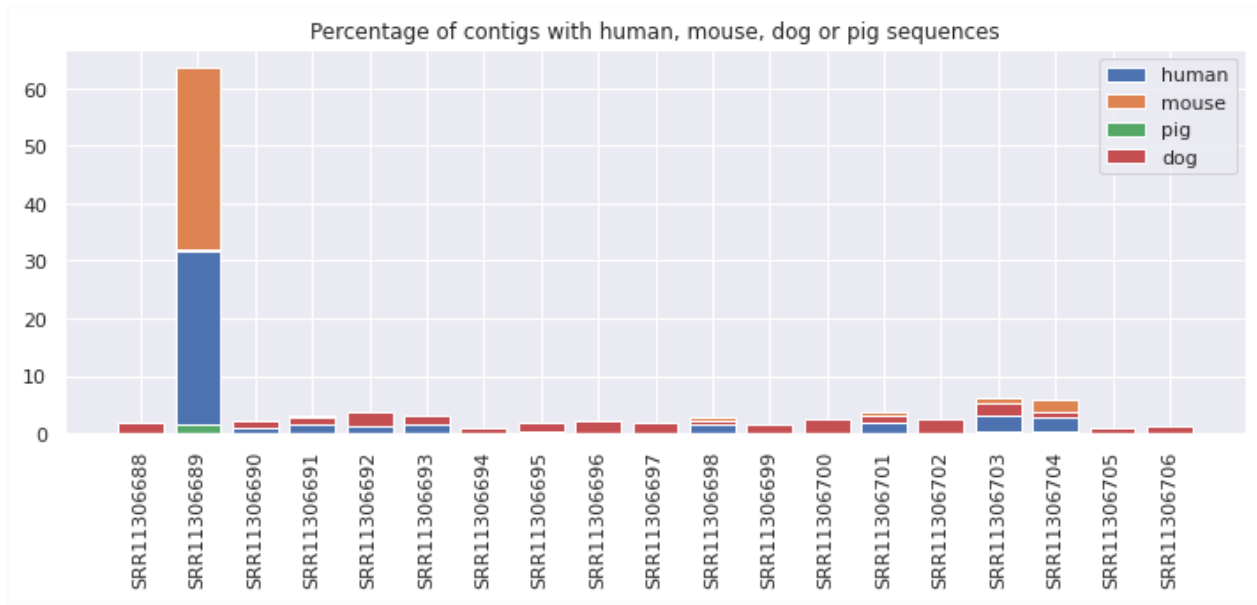


Fig 13. Percentage of contigs in each SRA in BioProject PRJNA610466 identified with ‘*homo sapiens*’ or ‘human’ (human), ‘*mus musculus*’ (mouse), ‘*sus scrofa*’ (pig) or ‘*canis lupus*’ (dog) sequences using MagicBLAST against a local copy of the nt database.

We identified an integration junction between a lentiviral vector and *Manis Pentadactyla* genomic DNA in contig k141_9009 in sample MJS3 (SRR11306689) using BLAST analysis against the NCBI nt database (Supp. Fig. S59-S62). In the same sample MJS3 we also identified a 3123-nt contig with a 98.28% identity to and 60% coverage for Lentiviral transfer vector FUW-tetO (MK318529.1) with an open reading frame with a 100% match for 694 nt to Expression vector pSOSV/ZsG-FL using BLAST analysis against the nt database (Supp Figs. S63-S65). In the same dataset we also identified sections of SV40 Large T antigen, widely used for cell immortalization (Supp. Fig. S66).

As per analysis of PRJNA573298 and PRJNA607174, we aligned the contigs to a local set of virus sequences downloaded from the Genome Sequence Archive using minimap2 (Supp info. 4.5). We found multiple contigs matching the following virus sequences: Synthetic Vaccinia virus clone GLV-1h68, Murine coronavirus, XMRV-like mouse endogenous retrovirus mERV-XL, Infectious bronchitis virus isolate YN/V90/2012 nucleocapsid protein-like (N) gene, Porcine epidemic diarrhea virus isolate GER/L03208/2019, Rous sarcoma virus, Moloney murine sarcoma virus, Cowpox virus, and numerous cloning and lentiviral vector sequences.

Liu et al. 2020 and Liu et al. 2021 (BioProject PRJNA686836): Pangolin CoV MP789

The pangolin CoV MP789 genome assembly was documented by Liu et al. (2020). After concerns over lack of data disclosure, particularity for gap filling, in Liu et al. (2020) raised by Chan and Zhan (2020), the sample GZ1-2 and ABIF raw chromatogram dataset

‘journal_ppat_1009664_s001’ were published by Liu et al. (2021). Using fastv for analysis of sample GZ1-2 (SRR13285085), we note a microbial profile distinct from other Guangdong Institute of Applied Biological Resources (GIABR) pangolin samples (Supp. Fig. S67,S68; Supp. Info. 5.2,5.3). We aligned the GZ1-2 dataset to the pangolin CoV MP789 genome using bowtie2 and bwa mem and note a low read count (271) and coverage (2.7%) (Table 4). In fact, this was a 76x lower read count and 10x lower genome coverage than for the Pacific flying fox faeces associated gemycircularvirus-1 (NC_038495.1) genome found in the dataset. Only 16 reads had any unique coverage (17 when using bwa mem for alignment), with each read repeated between 2 and 44 times. Furthermore no reads provided any additional MP789 genome coverage over pooled Lung07 and Lung08 samples (Liu et al. 2019), two of the three samples used by Liu et al. 2020 (Supp. Fig. S69). A plot of alignment of the journal_ppat_1009664_s001 amplicon dataset to the MP789 genome is shown in Supp Fig. S71.

Virus	N	Mean	Coverage%	Cov 4x %	Cov 10x %	Cov 30x %
MP789	271	17.01	2.69	2.52	2.2	0.34
phage M13	174	23.58	5.76	4.98	3.67	1.3
Tbat_A_103952	20719	1685.57	27.51	25.63	23.3	20.3
29_Fec80018_llama	543	193.19	6.36	5.74	5.56	5.56
Adeno-associated virus 5	86	24.16	3.84	3.84	2.31	1.08
BtRf-CV-8/NM2013	148	63.26	5.86	5.01	2.5	2.5
phage LKA1	426	13.75	3.72	3.1	2.31	0.24

Table 4. Coverage statistics for alignment using bowtie2 of sample GZ1-2 (SRR13285085) to the MP789 genome (MT121216.1) and other viruses identified with fastv. Statistics calculated using bamdst v1.0.9 and bamstats v1.25. N: number of reads mapped. Average depth calculated for mapped regions only. MP789: pangolin CoV MP789; For virus accessions and full descriptions see Supp Info. 0.4.

After *de novo* assembly, contigs were analysed against a local copy of the nt database using MagicBLAST. 2% of contigs had a best match to human sequences while 1.6% matched *Canis lupus* sequences (Supp. Fig. S70).

Rolling-circle read coverage

Circular read coverage was identified in Xiao et al. (2020) PRJNA607174 sample M1 (SRR11119759). Reads upstream (towards 5' end) of 505nt and downstream of 1204nt

consistently misaligned to Pangolin CoV MP789 (Fig. 16). We identified that when the reverse complement of the outlying sections of reads (423-504 nt and 1204-1284 nt) was taken, the resultant sequence then matched MP789 on the other side of this section of reads.



Fig. 14. Rolling circle reads in SRR11119759, reads aligned to MP789 using bwa mem and displayed in IGV. Misaligned sections of reads shown in strong colours.

Similarly, in Liu et al. (2019) sample Lung11 (SRR10168375) had significant sections of misalignment occur on 4 reads in the 16310-16694 nt region (Supp. Fig. S76). We found that for each of these reads (Supp. Info. 0.3 1-4), when the reverse complement of the misaligned section was analysed using BLASTN against the nt database, max score alignment was in each case MP789, with a maximum of one base mismatch, and alignment location was in the same 16310-16694 nt region. Similar read end misalignment/alignment of reverse complement of misaligned part to the MP789 genome was seen for 2 reads from Lung09 (SRR10168376) (Supp. Info. 0.3 ids 28,29) and multiple reads in SRR10168377 (Supp. Fig. S77, Supp. Fig. S78) and SRR10168378 (Supp. Fig. S79). Hassanin et al. (2020) interpreted that the circular read coverage was evidence for circular RNA molecules. However given the documented contamination and synthetic vectors in these datasets, and that circular RNAs are not generated by coronavirus RdRps, we believe a more likely explanation is that the circular reads are ligation-induced.

- 1) The level of SARS-r CoV reads in PRJNA573298 are low, with the maximum MP789 read counts were in Lung08, but these were 0.58X and 0.69X of the read counts for Great-Tit hosted Parus major densovirus reads in Lung19 and lymph01. While pangolin respirovirus isolate M5 virus read counts in sample Lung19 were 146x of the MP789 read counts in sample Lung08. The low level of reads in sample Lung08 (and even lower in the sample with next highest level, Lung07) are at a level that is most consistent with sample contamination rather than bona fide animal infection. We note that SARS-r CoV and MERS-r CoV contamination of sequencing datasets in China in 2017 and 2020 was documented by Zhang, D. et al. (2020), with SARS-r CoV read levels significantly higher than for MP789 in BioProject PRJNA573298.
- 2) The level of SARS-r CoV reads in PRJNA573298 are similar to read levels from mouse-hosted viruses: Murine type C retrovirus, *Mus musculus* mobilized endogenous polytropic provirus clone 15 truncated gag-pol polyprotein (gag) and envelope protein (env) genes as well as Great Tit hosted Parus major densovirus isolate PmDENV-JL (Yang et al. 2016).
- 3) Significant amounts of human and mouse sequences were identified using mitochondrial, STAT and MagicBLAST analysis against a local copy of the nt database of de novo assembled contigs. Each of the samples with pangolin CoV MP789 has both human and *Mus musculus* contamination, including the three samples with highest pangolin CoV MP789 read counts (Lung08,Lung07,Lung09) and as such the pangolin CoV MP789 reads could have been sourced from contamination by either of these potential host species.

Furthermore, in BioProject PRJNA573298, a moderate positive Spearman correlation coefficient of 0.6 was found between MP789 read and mouse contig counts (Supp. Fig. S11), which, when combined with the high levels of *Mus musculus* material, and numerous murine viruses observed in multiple datasets in PRJNA573298 (Fig. 2, Fig. 4, Supp. Info 1.1, 1.3) raises the possibility that the MP789 reads are mouse associated, potentially from human lung xenograft mouse material.

Lam et al. (2020) merged Guangdong pangolin scale dataset GD/P2S (SRR11093265) from BioProject PRJNA606875 with Lung12 (SRR10168374), Lung09 (SRR10168376), Lung08 (SRR10168377), Lung07 (SRR10168378) and Lung02 (SRR10168392) from BioProject PRJNA573298 to generate GD pangolin-CoV. However dataset GD/P2S contained 83 75nt long reads exactly matching, and 132 reads of 75-nt length with a single nucleotide difference to SARS-CoV-2 indicating a significant contamination issue with this dataset. Furthermore the dataset had an estimated 99.995% of the original reads filtered out and as such is not a true metagenomic sample that can be relied upon to verify the GD pangolin-CoV genome. We also note further contamination issues in datasets in BioProject PRJNA606875 with Vero-E6 based sample GX/P2V (SRR11093271) containing 20 reads of 70-95 nucleotide length exactly matching the SARS-CoV-2 genome and human and *Canis lupus* matching contigs identified from de novo assembly of sample GX/P3B (SRR11093270) .

The GD1 amplicon dataset (SRR13053879) published by Xiao et al. 2020 in their metagenomic analysis of lungs from the pangolins study contains pangolin CoV GD_1 (GISAID: EPI_ISL_410721) viral sequences embedded in synthetic vectors. This is most evident for reads aligned to the 3' and 5' ends of the pangolin CoV GD_1 genome where vector sequences are longest. Cloning vector pEASY-tub/hptII was identified as the vector used, with synthetic plasmids presumably sequenced rather than pangolin organ samples. No mention of the use of synthetic cloning or expression vectors was found in the methods section of Xiao et al. 2020. As the synthetically constructed GD1 amplicon dataset was provided as evidence for gap filling of the pangolin CoV GD_1 genome and the genome cannot be generated from the datasets in Xiao et al. (2020) Extended Data Table 3, pangolin CoV GD_1 cannot be relied upon to represent a true genome of a naturally occurring coronavirus infecting pangolins. The Xiao et al. 2020 paper and GD_1 genome sequence (GISAID: EPI_ISL_410721) therefore should be retracted.

Further indication of synthetic biology experimentation come from the identification of rolling circle reads containing both positive and negative strands at misaligned ends of reads across a 5 read wide zone in sample M1 (SRR11119759), which we interpret to be consistent with circularized cDNA generated during the ligation step of molecular cloning rather than naturally occurring circular RNA molecules (Hassanin et al. 2020). While the most complete example occurs in sample M1, several other occurrences of circular reads were identified in PRJNA573298. This indicates that synthetic data may be contained in raw WGS datasets in addition to the GD1 amplicons as described above.

In addition to synthetic vectors in amplicon dataset GD1, we identified significant contamination by non SARS-r CoV related synthetic vectors in PRJNA607174 with large African Swine Fever Virus and Porcine circovirus 2 contigs assembled, as well as vectors attached to several other viruses as per Supp info. 3.8.

Although we note that neither Pangolin respirovirus M5 or Pangolin CoV MP789 reads were found in this BioProject, the similar read levels of five contaminating viruses (Encephalomyocarditis virus, Moloney murine leukemia virus, Moloney murine sarcoma virus, Murine type C retrovirus, Mus musculus mobilized endogenous polytropic provirus clone 15 truncated gag-pol polyprotein (gag) and envelope protein (env) genes) and presence of Parus major densovirus isolate PmDENV-JL in both BioProject PRJNA610466 and BioProject PRJNA573298 indicates that samples from BioProject PRJNA573298 may have been used. This interpretation, however, is inconclusive. That we identified an integration junction between a lentiviral vector and *Manis Pentadactyla* genomic DNA in a contig as well as a Lentiviral transfer vector and SV40 Large T antigen in contigs potentially indicates that pangolin cell immortalization research was being undertaken by Li et al. (2020).

Datasets for sample GZ1-2 (SRR13285085) and amplicon dataset ‘journal_ppat_1009664_s001’ were published by Liu et al. 2021 after Chan and Zhan (2020) noted that the third dataset supporting the generation of the MP789 genome in Liu et al. 2020 and data for gap filling had not been published by Liu et al. 2020. Sample GZ1-2 had a very low MP789 read count, which was 76x lower than the read count for the clearly contaminating Pacific flying fox faeces associated gemycircularvirus-1 (NC_038495.1) genome. Given that the CoV reads are at a small fraction of contaminating sequences is more consistent for the MP789 to be from contamination than from infection of pangolins with a SARS-r CoV.

Pangolin CoV (both MP789 and GD_1) binding to pangolin ACE2 is tenfold weaker than binding to human ACE2 (Wrobel et al. 2021), which is consistent with the interpretation here that the reads in BioProject PRJNA573298 by Liu et al. 2019 stem from contamination, rather than from an evolutionary adaptation of a zoonotic virus to pangolins. Furthermore, pangolin CoVs (both MP789 and GD_1) exhibit comparable binding to hACE2 as SARS-CoV-2, yet no outbreaks of human infection by pangolin CoVs was reported among pangolin handlers (Choo et al. 2020). Laboratory contamination by hACE2-adapted SARS-r CoV experiments would be consistent with our findings. The RBM amino acid similarity between M789 and SARS-CoV-2 has led to multiple papers proposing recombination of a progenitor virus with the RBD of Guangdong pangolin CoV (MP789/GD_1 or genome generated directly from Liu et al. 2019) as the source for SARS-CoV-2 (Andersen et al. 2020; Li X et al. 2020b; Makarenkov et al. 2021). However, here we speculate the hypothesis that the RBM for M789 could possibly have been used as a progenitor for this part of the SARS-CoV-2 virus.

In a longitudinal survey of 334 pangolins in Malaysia (Lee et al. 2020) failed to find any evidence of coronaviruses or other potentially zoonotic viruses in pangolins in the wild. Similarly, in a metagenomic study, Hu et al. (2020) did not find any SARS-CoV-2 related reads in samples from one Malayan pangolin collected in 2017. Furthermore, Zhang (2020) did not find any reads matching pangolin CoV sequences in 93 pangolin samples from Hu et al. (2020) BioProject PRJNA529540. Here we failed to find any trace of coronavirus sequences from 7 *M. javanica* pangolins collected from the Guangdong Provincial Wildlife Rescue Centre in BioProject PRJNA610466 (Li H. et al. 2020). While Wenzel (2020) and Choo et al. (2020) propose humans may have been the source of the infection by pangolin CoV (GD_1/MP789), the 90.32% (Liu et al. 2020) of the MP789 genome/91.02% (Xiao et al. 2020) similarity of the GD_1 genome to SARS-CoV-2 is sufficiently different that pangolin CoV MP789 could not have evolved during the pangolins time in captivity. In summary, our findings are consistent with a single source of pangolins with pangolin CoV MP789/GD_1 (Chan and Zhan, 2020), and given the contamination and synthetic vectors identified in the pangolin datasets discussed here, we believe the most parsimonious explanation for the occurrence of SARS-r CoV reads in pangolin datasets is that they were derived from contamination from hACE2 adapted SARS-r CoV experimentation. That pangolin CoV MP789/GD_1 has been widely used for SARS-CoV-2

origins studies is concerning and we urge all published studies relying on these pangolin CoVs to review their work in light of our findings.

Conclusion

We have documented frequent and abundant contamination of pangolin metagenomic samples with sequences from multiple potential coronavirus host species, dominantly human and *Mus musculus* sequence contamination. We further document numerous non-pangolin hosted virus sequences, many in higher abundance than coronavirus sequences. Indeed in the main dataset generated by Liu et al. (2019) from which the bulk of pangolin coronavirus genomes GD_1 and MP789 were derived, SARS-r CoV reads are fewer than bird hosted Parus Major densovirus and rodent virus Encephalomyocarditis virus which is commonly pig hosted. While two murine virus read levels are higher for all but two pangolin samples containing SARS-r CoV sequences. In the datasets provided by Xiao et al. (2020) we identified African Swine Fever Virus, Simian Virus 40, Gemycircularvirus SL1 and bacteriophages M13 and DE3 in higher abundance than SARS-r CoV reads. We also find numerous contigs of laboratory cloning vectors with viral sequences embedded in multiple BioProjects, all of which indicate that pangolins were not infected by naturally occurring coronaviruses, but that the SARS-r CoV reads found in multiple datasets were more likely contamination related. Finally, we document pangolin coronavirus sequences embedded in synthetic cloning vectors in the GD1 amplicon dataset (SRR13053879), which further suggests the coronavirus sequences identified in the pangolin samples were laboratory related and not from naturally occurring pangolin viruses.

Methods

Cleaning

Reads in SRA datasets in BioProject PRJNA573298, PRJNA606875, PRJNA607174, PRJNA610466 and PRJNA686836 were trimmed and filtered using fastp with default settings.

Fastv microbial analysis

All SRA's in BioProjects PRJNA573298, PRJNA606875, PRJNA607174, PRJNA610466, and PRJNA686836 were analysed against the Opengene viral genome kmer collection 'microbial.kc.fasta.gz' (<https://github.com/OpenGene/UniqueKMER>) downloaded on the 7/3/2021, using fastv (Chen et al. 2020). Results can be found in Supp. Info. 1.2, 2.2, 3.2, 4.2, 5.1.

Alignment to specific viral sequences

Several virus gene sequences were identified using fastv to have significant abundance (>~100 k-mer hits) across SRA's in BioProjects PRJNA573298, PRJNA606875, PRJNA607174, PRJNA610466, and PRJNA686836. Fastp cleaned reads were then aligned to selected virus

genomes using either bowtie2 version 2.4.2 (Langmead and Salzberg, 2012), bwa mem version 0.7.17 (Li, 2013) or bwa mem2 version 2.0 (Vasimuddin et al. 2019) using default parameters. GATK version 4.1.9.0 (Van der Auwera & O'Connor, 2020) was used to sort then mark duplicates. Samtools version 1.11 (Li et al. 2009) was used to index the marked .bam files for viewing in IGV version 2.8.13 (Thorvaldssdóttir et al. 2013) (Supp. Info. 1.4, 1.5; 2.4, 2.5; 3.3, 3.4; 4.3, 4.4; 5.2)

Soft-clipped read end BLAST analysis.

For amplicon dataset GD_1, we aligned the reads with bwa-mem2 to MT121216.1 using the -Y parameter. We then extracted the soft-clipped sections greater than 14 bases long at read ends for both 5' and 3' ends. We then used local BLAST to query each soft-clipped section against the nt database using percentage identity 95% and expect value of 0.001.

De novo assembly

Fastp cleaned reads from each whole-genome sequencing (WGS) SRA in PRJNA573298, PRJNA606875, PRJNA607174, PRJNA610466 and PRJNA686836 were de novo assembled using MEGAHIT v1.2.9 (Li et al., 2015) with default parameters. Amplicon dataset SRR13053879 was de novo assembled using MEGAHIT with the following parameters: --k-max 79 --k-step 10.

MagicBLAST alignment

Each de novo assembled contig in PRJNA573298, PRJNA606875, PRJNA607174, PRJNA610466 and PRJNA686836 was analysed using MagicBLAST by querying each contig against the a local copy of the nt database using default parameters. For Supp. Info. 2.3 for PRJNA606875, *Manis javanica*, *Manis pentadactyla* and *Manis tricuspis* gene RNA and DNA sequences were filtered out from results to reduce file size.

Primer and vector identification

Each de novo assembled contig in PRJNA573298, PRJNA606875, PRJNA607174, PRJNA610466 and PRJNA686836 was queried against common primer and promoter sequences to identify potential synthetic constructs. Further, *de novo* assembled contigs were analysed using MagicBLAST, querying the contig against a local copy of the NCBI nt database (downloaded on 21/1/2021). Contigs with an accession description with specific text sequences e.g 'vector' were saved to separate files.

Adapter identification

For amplicon dataset GD1 (SRR13053879) we searched for the first 12 or 13nt of the following adapter sequences in the file: Illumina: AGATCGGAAGAGC; Small RNA: TGGAATTCTCGG; Nextera: CTGTCTCTTATA. None were detected.

Taxonomic analysis and species identification

Multiple methods were used for taxonomic analysis. Each SRA in PRJNA573298, PRJNA606875, PRJNA607174, PRJNA610466 and PRJNA686836 was analysed using the online NCBI STAT tool to identify the lowest common taxonomical node for each read.

SRA's in PRJNA573298, PRJNA606875, PRJNA607174, PRJNA686836 and PRJNA610466 were aligned to the mitochondria from Homo sapiens (NC_012920.1), Manis pentadactyla (MT335859.1), Manis javanica (MG196309.1), Mus musculus (KY018919.1) Chlorocebus aethiops (MN816163.1), Macaca mulatta (NC_005943.1), Rhinolophus sinicus (KP257597.1), Pipistrellus abramus (KX355640.1), Rhinolophus affinis (NC_053269.1), Sus scrofa (MK251046.1) and Canis lupus familiaris (MW549038.1) using bowtie2 with default parameters.

Local BLAST

Local BLAST (Camacho et al. 2009) analysis was conducted using NcbiblastnCommandline in BioPython using expect value=0.001 and percentage identity of 0.95.

Minimap alignment

Contigs in PRJNA573298, PRJNA607174 and PRJNA610466 were aligned to a database of viruses downloaded from the Genome Sequence Archive on the 1/3/2021 using minimap2 version 2.20 (Li H. 2018).

Acknowledgements

We thank Prof. Virginie Courtier, Francisco de Asis, and an anonymous reviewer for discussion and feedback which helped improve this manuscript.

References

- Agostini ML, Pruijssers AJ, Chappell JD, et al. Small-Molecule Antiviral ⁿ-D-N4-Hydroxycytidine Inhibits a Proofreading-Intact Coronavirus with a High Genetic Barrier to Resistance. 2019;(October):1-14.
- Andersen KG, Rambaut A, Lipkin WI, Holmes EC, Garry RF. The proximal origin of SARS-CoV-2. Nat Med. 2020;26(4):450-452. doi:10.1038/s41591-020-0820-9
- Bai J, Lin H, Li H, et al. Cas12a-Based On-Site and Rapid Nucleic Acid Detection of African Swine Fever. Front Microbiol. 2019;10(December):1-9. doi:10.3389/fmicb.2019.02830

Camacho C, Coulouris G, Avagyan V, et al. BLAST+: architecture and applications. *BMC Bioinformatics*. 2009;10(1):421. doi:10.1186/1471-2105-10-421

Chan YA, Zhan SH. Single source of pangolin CoVs with a near identical Spike RBD to SARS-CoV-2. Published online 2020:1-15. doi:10.1101/2020.07.07.184374

Chen S, He C, Li Y, Li Z, Melançon CE. A computational toolset for rapid identification of SARS-CoV-2, other viruses and microorganisms from sequencing data. *Brief Bioinform*. 2020;00(August):1-12. doi:10.1093/bib/bbaa231

Choo SW, Zhou J, Tian X, et al. Are pangolins scapegoats of the COVID-19 outbreak-CoV transmission and pathology evidence? *Conserv Lett*. 2020;13(6):1-12. doi:10.1111/conl.12754

Cuevas JM, González-Candelas F, Moya A, Sanjuán R. Effect of Ribavirin on the Mutation Rate and Spectrum of Hepatitis C Virus In Vivo. *J Virol*. 2009;83(11):5760-5764. doi:10.1128/jvi.00201-09

Deigin Y, Segreto R. SARS-CoV-2's claimed natural origin is undermined by issues with genome sequences of its relative strains: Coronavirus sequences RaTG13, MP789 and RmYN02 raise multiple questions to be critically addressed by the scientific community. *BioEssays*. 2021;43(7). doi:10.1002/bies.202100015

Gao W-H, Lin X-D, Chen Y-M, et al. Newly identified viral genomes in pangolins with fatal disease. *Virus Evol*. 2020;6(1). doi:10.1093/ve/veaa020

Hassanin A. The SARS-CoV-2-like virus found in captive pangolins from Guangdong should be better sequenced. Published online 2020:3-8.

Hassanin A, Jones H, Ropiquet A. SARS-CoV-2-like viruses from captive Guangdong pangolins generate circular RNAs. *Nature*. Published online 2020. <https://hal.archives-ouvertes.fr/hal-02616966/>

Hu JY, Hao ZQ, Frantz L, et al. Genomic consequences of population decline in critically endangered pangolins and their demographic histories. *Natl Sci Rev*. 2020;7(4):798-814. doi:10.1093/NSR/NWAA031

Huang Z, Gong L, Zheng Z, et al. GS-441524 inhibits African swine fever virus infection in vitro. *Antiviral Research*, 2021, 191, 105081. <https://doi.org/10.1016/j.antiviral.2021.105081>

Lam, T. T. Y., Shum, M. H. H., Zhu, H. C., Tong, Y. G., Ni, X. B., Liao, Y. S., Wei, W., Cheung, W. Y. M., Li, W. J., Li, L. F., Leung, G. M., Holmes, E. C., Hu, Y. L., Guan, Y. (2020). Identification of 2019-nCoV related coronaviruses in malayan pangolins in southern China. *BioRxiv*. <https://doi.org/10.1101/2020.02.13.945485>

Lee J, Hughes T, Lee M-H, et al. No Evidence of Coronaviruses or Other Potentially Zoonotic Viruses in Sunda pangolins (*Manis javanica*) Entering the Wildlife Trade via Malaysia. *Ecohealth*. 2020;17(3):406-418. doi:10.1007/s10393-020-01503-x

Li H. 2013. bwa-mem. <http://bio-bwa.sourceforge.net/bwa.shtml#13>

Li H. Minimap2: Pairwise alignment for nucleotide sequences. *Bioinformatics*. 2018;34(18):3094-3100. doi:10.1093/bioinformatics/bty191

Li HM, Liu P, Zhang XJ, et al. Combined proteomics and transcriptomics reveal the genetic basis underlying the differentiation of skin appendages and immunity in pangolin. *Sci Rep*. 2020;10(1):1-13. doi:10.1038/s41598-020-71513-w

Li X, Xiao K, Chen X, et al. Pathogenicity, tissue tropism and potential vertical transmission of SARS-CoV-2 in Malayan pangolins. 2020a. *BioRxiv* 2020. doi:10.1101/2020.06.22.164442

Li X, Giorgi EE, Marichannegowda MH, et al. Emergence of SARS-CoV-2 through recombination and strong purifying selection. 2020b. *Sci Adv*. 2020;6(27):eabb9153. doi:10.1126/sciadv.abb9153

Liu P, Chen W, Chen JP. Viral metagenomics revealed sendai virus and coronavirus infection of malayan pangolins (*manis javanica*). *Viruses*. 2019;11(11). doi:10.3390/v11110979

Liu P, Jiang J-Z, Wan X-F, Hua Y, Li L., Zhou J, Wang, X, Hou, F, Chen, J, Zou, J, Chen, J. (2020). Are pangolins the intermediate host of the 2019 novel coronavirus (SARS-CoV-2)? *PLOS Pathogens*, 16 (5), e1008421. <https://doi.org/10.1371/journal.ppat.1008421>

Liu P, Jiang J-Z, Wan X-F, et al. Correction: Are pangolins the intermediate host of the 2019 novel coronavirus (SARS-CoV-2)? *PLOS Pathog*. 2021;17(6):e1009664. doi:10.1371/journal.ppat.1009664

Makarenkov V, Mazoure B, Rabusseau G, Legendre P. Horizontal gene transfer and recombination analysis of SARS-CoV-2 genes helps discover its close relatives and shed light on its origin. *BMC Ecol Evol*. 2021;21(1):1-18. doi:10.1186/s12862-020-01732-2

Matyasek R, Kovarik A. Mutation patterns of human SARS-COV-2 and bat RaTG13 coronaviruses genomes are strongly biased towards C>U indicating rapid evolution in their hosts. 2020;(April). doi:10.21203/rs.3.rs-21377/v1

Niu S, Wang J, Bai B, et al. Molecular basis of cross-species ACE2 interactions with SARS-CoV-2-like viruses of pangolin origin. EMBO J. Published online 2021:1-12. doi:10.15252/embj.2021107786

Sims D, Sudbery I, Illott NE, Heger A, Ponting CP. Sequencing depth and coverage: Key considerations in genomic analyses. Nat Rev Genet. 2014;15(2):121-132. doi:10.1038/nrg3642

Vasimuddin Md, Sanchit Misra, Heng Li, Srinivas Aluru. Efficient Architecture-Aware Acceleration of BWA-MEM for Multicore Systems. IEEE Parallel and Distributed Processing Symposium (IPDPS), 2019.

Wei C, Lin Z, Dai A, et al. Emergence of a novel recombinant porcine circovirus type 2 in China: PCV2c and PCV2d recombinant. Transbound Emerg Dis. 2019;66(6):2496-2506. doi:10.1111/tbed.13307

Wenzel J. Origins of SARS-CoV-1 and SARS-CoV-2 are often poorly explored in leading publications. Cladistics. 2020;36(4):374-379. doi:10.1111/cla.12425

Wrobel AG, Benton DJ, Xu P, et al. Structure and binding properties of Pangolin-CoV spike glycoprotein inform the evolution of SARS-CoV-2. Nat Commun. 2021;12(1):837. doi:10.1038/s41467-021-21006-9

Wu K, Liu J, Wang L, et al. Current state of global african swine fever vaccine development under the prevalence and transmission of ASF in China. Vaccines. 2020;8(3):1-26. doi:10.3390/vaccines8030531

Xiao K, Zhai J, Feng Y, et al. Isolation of SARS-CoV-2-related coronavirus from Malayan pangolins. Nature. 2020;583(7815):286-289. doi:10.1038/s41586-020-2313-x

Yang et al. 2016. Genetic characterization of a densovirus isolated from great tit (*Parus major*) in China. <https://doi.org/10.1016/j.meegid.2016.03.035>

Yang R, Peng J, Zhai J, et al. Pathogenicity and transmissibility of a novel respirovirus isolated from a Malayan pangolin. J Gen Virol. 2021;102(4). doi:10.1099/jgv.0.001586

Yang WT, Shi SH, Jiang YL, et al. Genetic characterization of a densovirus isolated from great tit (*Parus major*) in China. *Infect Genet Evol.* 2016;41:107-112.
doi:10.1016/j.meegid.2016.03.035

Zhai SL, Chen SN, Xu ZH, et al. Porcine circovirus type 2 in China: An update on and insights to its prevalence and control. *Virology*. 2014;11(1):1-13. doi:10.1186/1743-422X-11-88

Zhai SL, Zhou X, Lin T, et al. Reappearance of buffalo-origin-like porcine circovirus type 2 strains in swine herds in southern China. *New Microbes New Infect.* 2017;17:98-100.
doi:10.1016/j.nmni.2017.02.009

Zhang T, Wu Q, Zhang Z. Probable Pangolin Origin of SARS-CoV-2 Associated with the COVID-19 Outbreak. *Curr Biol.* 2020;30(7):1346-1351.e2. doi:10.1016/j.cub.2020.03.022

Zhang, D. The Pan-SL-CoV/GD sequences may be from contamination. 2020. Zenodo doi: 10.5281/zenodo.5004213

Zhang D, Jones A, Deigin Y, Sirotkin K, Sousa A, Mccairn K. Unexpected Novel Merbecovirus Discoveries in Agricultural Sequencing Datasets from Wuhan, China. 2021. arXiv:2104.01533 [q-bio.GN]

Supplementary material

All supplementary material including the files listed below can be accessed at
doi: 10.5281/zenodo.5235662

Link: <https://zenodo.org/record/5235662>

Supp. Figs.

Supp_Figs.pdf

Supp Info.

0_Datasets.xlsx

1_PRJNA573298_analysis.xlsx

2_PRJNA606875_analysis.xlsx

3_PRJNA607174_analysis.xlsx

4_PRJNA610466_analysis.xlsx

5_PRJNA686836_analysis.xlsx

Supp Data

Porcine circovirus 2 contig: SRR11119762_k141_294696.fa

ASFV contig: SRR11119764_k141_1503693.fa

Coning vector: SRR13053879_pEASY-T1_from_spliced_read_ids_21_25.fa

Genomic DNA junction: SRR11306689_k141_9009

GD1 amplicon contigs K79_3, K79_5: SRR13053879_k79_3_k79_5.fa

Code

https://github.com/bioscienceresearch/Pangolin_CoV_SRA_analysis